Constraints on the binary black hole hypothesis for system LB-1

Rong-Feng Shen,[1, *] Christopher D. Matzner,[2] Andrew W. Howard,[3] and Wei Zhang[4]

[1]*School of Physics and Astronomy, Sun Yat-Sen University, Zhuhai, 519082, China*
[2]*Department of Astronomy and Astrophysics, University of Toronto, Toronto, ON M5S 3H4, Canada*
[3]*Department of Astronomy, Caltech, Pasadena, CA 91125, USA*
[4]*Key Laboratory of Optical Astronomy, National Astronomical Observatories, CAS, Beijing 100101, China*

ABSTRACT

At about 70 solar masses, the recently-discovered dark object orbited by a B-type star in the system LB-1 is difficult to understand as the end point of standard stellar evolution, except as a binary black hole (BBH). LB-1 shows a strong, broad H-alpha emission line that is best attributed to a gaseous disk surrounding the dark mass. We use the observed H-alpha line shape, particularly its wing extension, to constrain the inner radius of the disk and thereby the separation of a putative BBH. The hypothesis of a current BBH is effectively ruled out on the grounds that its merger time must be a small fraction of the current age of the B star. The hypothesis of a previous BBH that merged to create the current dark mass is also effectively ruled out by the low orbital eccentricity, due to the combination of mass loss and kick resulted from gravitational wave emission in any past merger. We conclude that the current dark mass is a single black hole produced by the highly mass-conserving, monolithic collapse of a massive star.

Keywords: stellar mass black holes – H I line emission – stellar accretion disks – late stellar evolution – gravitational wave sources

1. INTRODUCTION

Liu et al. (2019) recently discovered the LB-1 system during a radial velocity (RV) monitoring search for spectroscopic binaries containing black hole (BH) candidates. Located toward the Galactic anti-center, LB-1 consists of a B-type star with a RV period of $P = 79$ d. Spectroscopic analysis suggests that its luminous component is a sub-giant with a mass $M_B \approx 8 M_\odot$, a radius of $9 R_\odot$, a metallicity of $1.2 Z_\odot$, and an age $t_B \approx 35$ Myr. The fit to the spectral energy distribution from U, B and V photometry yields a distance of 4.2 kpc. The fit to its RV curve gives a semi-amplitude $K_B = 52.8 \pm 0.7$ km/s and an eccentricity $e = 0.03 \pm 0.01$, thus a mass function $P K_B^3 / 2\pi G = 1.20 \pm 0.05 M_\odot$, suggesting the unseen companion has a mass of at least $6 M_\odot$ (for edge-on view), making it a BH candidate.

More importantly, LB-1 shows a prominent, broad (FWHM= 240 km/s) Hα emission line (shown in Figure 1) which moves in anti-phase with the B star at a much smaller semi-amplitude $K_\alpha = 6.4 \pm 0.8$ km/s. These properties rule out a circum-binary nebula or a disk associated with the B star as the origin of the Hα line,

but they are consistent with a gaseous disk around the BH candidate (Liu et al. 2019). In this case, RV amplitude ratio $K_B/K_\alpha = M_{BH}/M_B$ immediately gives a BH mass $M_{BH} = 68^{+11}_{-13} M_\odot$, requiring a near-polar inclination $i \approx 15°$-$18°$ (Liu et al. 2019).

Such a large BH mass poses a challenge to current theories about BH formation and final-stage evolution of massive stars, as Leung et al. (2019) find that the pulsational pair-instability mass ejection before the final supernova explosion sets a maximum mass of BHs to be $\sim 50\ M_\odot$.

One attractive possibility that could partially alleviate these challenges is that the primary in LB-1 is not a single, but a binary of BHs (a BBH). This would have interesting implications for gravitational wave sources. In this *Letter* we consider this possibility and put constraints on it from the observed properties of LB-1's Hα emission line (§2), as well as from the consequence of any prior BH merger event (§3). Conclusions are given in §4.

2. CONSTRAINT FROM THE Hα LINE

The possibility of a current BBH is strongly constrained by the maximum coalescence time implied by the inner radius of Hα disk, which in turn is constrained
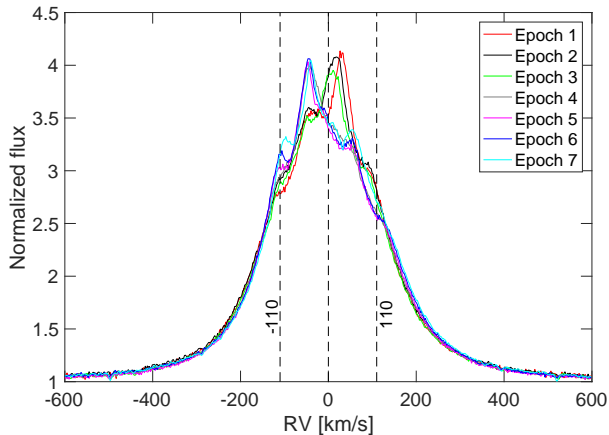
* shenrf3@mail.sysu.edu.cn

Figure 1. Keck high-resolution multi-epoch data of the Hα emission line shape from LB-1. The data set are used in Liu et al. (2019)

.

by the shape of the Hα line. We begin with a general consideration of the kinematic information conveyed by a generic disk emission line, before constraining the inner and outer radii of the disk in LB-1.
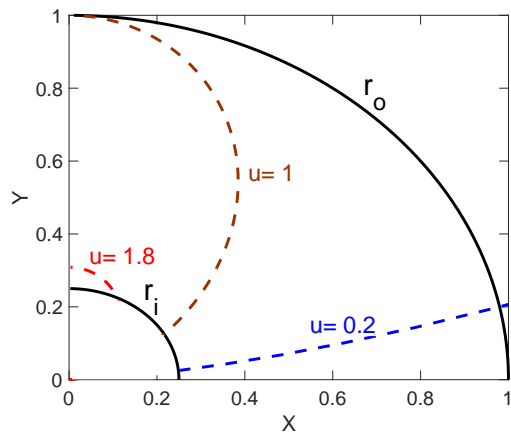

Figure 2. The illustration showing one quarter of the Hα-emitting disk. The colored dashed lines mark the regions with constant line-of-sight velocity component u. The disk outer radius r_o is set to be 1, and u is set to be 1 for $\theta = \pi/2$ at r_o.

2.1. Kinematically broadened line shape

We assume the emission line's thermal width is much smaller than the kinematically broadened line width, so the intrinsic line shape can be taken as a δ-function. Consider a thin Keplerian disk with an inner radius R_i, an outer radius R_o, and an inclination angle i. On the

disk's outer rim the largest line-of-sight velocity component (radial velocity) is $v_0 = (GM/R_o)^{1/2} \sin i$, where M is the central object's mass. Let θ be the azimuthal angle on the disk plane, and $\theta = 0$ corresponds to the projected location of the observer's line of sight.

Let $r = R/R_o$ be the dimensionless radius, and $u(r, \theta)$ be the local radial velocity on the disk, normalized by v_0; then

$$u = r^{-1/2} \sin \theta. \tag{1}$$

Note that $0 \leq u \leq u_{\max}$ where $u_{\max} = r_i^{-1/2}$.

The observed line emission flux F within the velocity interval $(u, u + du)$ is (Smak 1969, 1981; Huang 1972; Horne & Marsh 1986)

$$F(u)du = \iint_{D(u)} j(r)\, r dr d\theta, \tag{2}$$

where $j(r)$ [erg s^{-1} cm^{-2}] is the line emissivity function; we will simply take it as a power law function $j(r) \propto r^{-a}$. The integral region $D(u)$ on the disk is given by

$$u \leq r^{-1/2} \sin \theta \leq u + du. \tag{3}$$

Note that $F(u)$ is symmetric at $\pm u$. Also, the two quarters $0 < \theta < \pi/2$ and $\pi/2 < \theta < \pi$ contribute equally to $F(u)$, so we consider the first quarter only in computing the integral, then later multiply the result by 2. The dashed line in Figure 2 illustrate $D(u)$ for three u values, respectively.

To carry out the double integral, we first do the integral over θ with r being fixed. Change the differential variable using eq. (1):

$$d\theta = \frac{d(\sin \theta)}{\sqrt{1 - u^2 r}} = \frac{r^{1/2}\, du}{\sqrt{1 - u^2 r}}, \tag{4}$$

then eq. (2) becomes

$$\begin{aligned} F(u)du &= 2 \int j(r) dr \int_{ur^{1/2}}^{r^{1/2}(u+du)} \frac{d\sin \theta}{\sqrt{1 - u^2 r}} \\ &= 2\, du \int \frac{j(r) r^{3/2}\, dr}{\sqrt{1 - u^2 r}}. \end{aligned} \tag{5}$$

Thus,

$$F(u) = 2 j(r_o) \int_{r_i}^{\min(1/u^2, 1)} \frac{r^{3/2 - a}\, dr}{\sqrt{1 - u^2 r}}. \tag{6}$$

Note that when $u > u_{\max}$, the upper limit of the integral will be $< r_i$, then one has to set $F(u) = 0$. For ease of computation, change the variable: let $x \equiv r^{1/2} u$. Then,

$$F(u) = 4 j(r_o) u^{2a-5} \int_{x_i}^{x_o} \frac{x^{4-2a}\, dx}{\sqrt{1 - x^2}}, \tag{7}$$

where $x_i = r_i^{1/2} u$ and $x_o = \min(1, u)$. Again, when $u \geq u_{\max}$, $F(u)$ shall be set to 0.
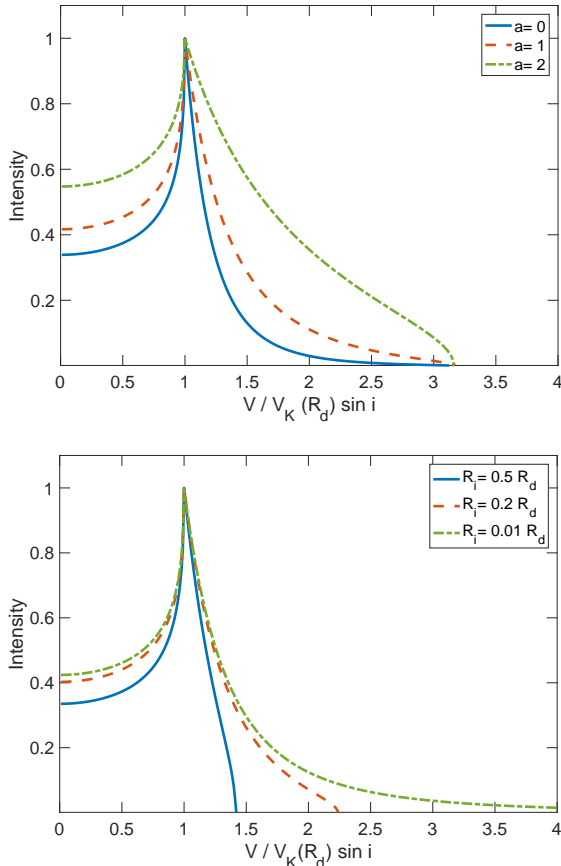
Figure 4. Model fit of equation (7) to the Keck epoch 2 data.

Figure 3. The dependence of the line shape, computed from equation (7), on the emissivity's radial index a (*top*) and on the disk's inner radius r_i (*bottom*).

2.2. *Model parameter dependence*

Equation (7) is for the case in which the disk is optically thin to the line photons. It produces a well known double-peak line profile which peaks symmetrically at $u = \pm 1$ (i.e., RV$= \pm v_0$, e.g., Huang 1972). The shape of the line wings is determined by how the emissivity varies radially and how far the disk extends inward. Smak (1969, 1981) investigated the line profile's dependence on a and r_i, finding that a controls the slope of the wings and r_i determines their extension (as $u_{\max} = r_i^{-1/2}$), as we reproduced in Figure 3.

LB-1's emission line shows a central peak with shoulders, the so-called "wine-bottle" shape seen in some Be stars. According to Hummel & Dachs (1992) and Hummel (1994), this type of line shape is due to a combination of non-coherent scattering and kinematic broadening, and appears only at low inclination angles ($i \sim 5°-20°$) and only when the disk is optically thick at the line center. For optically thin cases, the wine-bottle shape is replaced by the classical double-peak profile.
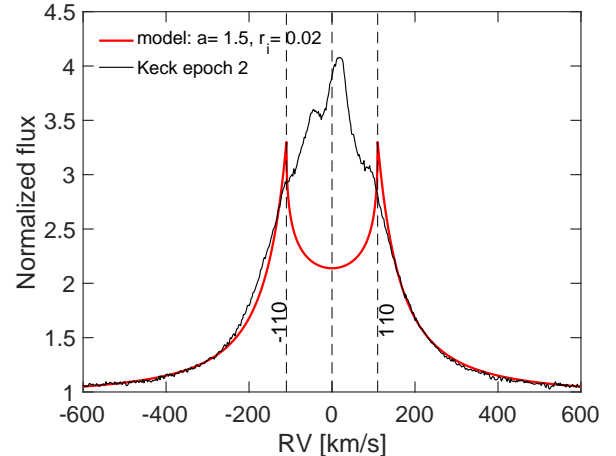
Reproducing the wine-bottle shape seen in LB-1 requires a three-dimensional radiative line-transfer computation, which is beyond the scope of this Letter. Nevertheless, results from such a computation by Hummel (1994, their Fig. 7) show that, for disks with the same geometrical properties, the RV positions of the shoulders of the wine-bottle shape for the optically thick case are the same as those of the double peaks in the optically thin case. Therefore, the shoulder positions still indicate the outer disk radius. Furthermore, the physical correspondence of the wing extension and slope with r_i and a, respectively, is likewise preserved.

2.3. *Constraint on disk inner radius*

In Figure 4 we show a model fit to LB-1's line shoulder positions and the wing shape. We used the data from one observation epoch only, because the shoulder position and wind shape do not vary much among epochs (see Figure 1). The observed RV is $v = v_K \sin i$, where $v_K = \sqrt{GM/R}$. In modeling we have taken the dark primary mass $M = 68 M_\odot$ and the inclination $i = 16°$ reported in Liu et al. (2019).

For the observed RVs of line shoulder $v_{\mathrm{sho}} = 110$ km s^{-1} and line extension $v_{\mathrm{ext}} \geq 600$ km s^{-1}, the outer and inner radii of the Hα-emitting region of the disk are

$$R_o = 0.38 \,\mathrm{AU}, \quad R_i \leq 0.013 \,\mathrm{AU} = 2.8 \, R_\odot, \quad (8)$$

respectively. Note that 0.013 AU is only an upper bound for the disk inner radius R_i, as the real R_i could be even smaller if the innermost region is ionized.

The inferred inner disk radius strongly constrains the possibility that the central dark primary is composed of a binary of BHs with a total mass M. Due to gravitational interaction, such a binary would truncate the

circum-binary disk at a radius that is 1.7 times the semi-major axis a_b of the binary when the binary orbit is circular; a higher eccentricity would cause a larger inner gap to the disk (Artymowicz & Lubow 1994). Therefore, $a_b \approx R_i/1.7 \leq 1.6\,R_\odot$. Assuming a circular orbit, the in-spiral time of such a binary due to gravitational wave emission is (Peters 1964)

$$
\begin{aligned}
T(a_b) = \frac{5c^5 a_b^4}{256 G^3 M^2 \mu} &\lesssim 1.3 \times 10^4 \\
&\times \left(\frac{a_b}{1.6\,R_\odot}\right)^4 \left(\frac{68\,M_\odot}{M}\right)^3 \left(\frac{M/4}{\mu}\right) \text{yr},
\end{aligned}
\quad (9)
$$

where the reduced mass μ takes a value of $M/4$ for the equal-mass case of the binary. A higher eccentricity would make this time even shorter.

This in-spiral time is characteristically more than 3 orders of magnitude shorter than the B star age $t_B \sim 35$ Myr, which strongly disfavors the possibility of a current central black hole binary. Indeed, the system would be obscured by its proto-stellar envelope if it were younger than $\sim 10^5$ years. A non-equal binary does not alleviate this constraint, as the mass ratio would have to exceed 10^3 to make the in-spiral time comparable to the lifespan of a B star.

3. A PAST MERGER OF BINARY BLACK HOLES

Could it be that the merger of a binary of BHs (BBH) had happened long ago? The low observed eccentricity of the LB-1 system severely limits this possibility, as the effects of gravitational radiation would tend to excite much higher eccentricities, or unbind the system entirely.

First, consider the loss of total mass in a BBH merger due to radiated energy. Liu et al. (2019) infer that the gravitating mass of LB-1 cannot have changed by more than 4% in a single orbit of the B star, without increasing the eccentricity above its observed value. Barausse, Morozova, & Rezzolla (2012) present a highly accurate formula for the radiated energy, which we display in Figure 5 for the cases of maximal spins aligned or anti-aligned with the BBH orbit, as well for the case of no net spin alignment, as functions of the greater component mass of the BBH. From this, it is clear that, for less than 4% of the mass to be radiated and both components to be less than $50\,M_\odot$, it requires some spin-orbit anti-alignment ($\tilde{a} < 0$ in Barausse's terminology), although there is a narrow window around $47\,M_\odot$ in which no spin is necessary.

Note, however, that gravitational wave recoil is a generic outcome of BBH mergers, which tends to introduce a high eccentricity to system, or might even dissociate it. For a circularly orbiting binary of Schwarzschild
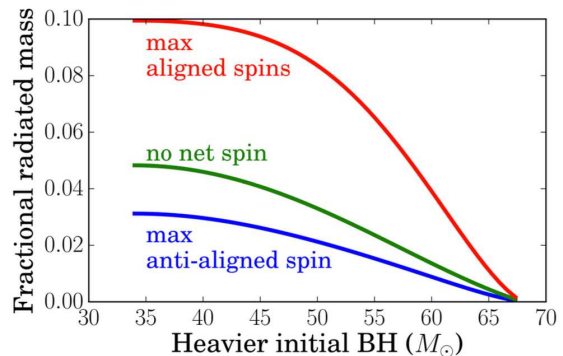

Figure 5. The fractional radiated mass during a BBH merger as a function of the primary BH mass, using the model of Barausse, Morozova, & Rezzolla (2012) and assuming a total mass of $68\,M_\odot$. The red, green, and blue lines represent maximal spins aligned with the BBH orbital axis, no net spin, and maximally anti-aligned spins, respectively.

BHs, Fitchett (1983) provides a quasi-Newton estimate for the recoil velocity of the merged BH, which is equivalent to

$$
v \approx 1000 \frac{q^2(1-q)}{1+q} \text{ km/s}, \quad (10)
$$

which takes a maximum of about $91\,\text{km/s}$ when the mass ratio $q = (\sqrt{5} - 1)/2$. Advanced calculations including numerical relativity simulations taking into account black hole spins suggest the recoil velocity is typically $v \approx 10^{-3}c = 300\,\text{km/s}$ (Gerosa, Hébert & Stein 2018); and in the extreme case of maximal anti-aligned spins in a binary with $q = 0.623$, the recoil can reach $526\,\text{km/s}$ (Healy et al. 2014). Considering that the circular velocity of the LB-1 system is about $100\,\text{km/s}$ (Liu et al. 2019), a kick of only a few km/s would create a greater eccentricity than what is observed. Although it is possible to arrange for zero kick, for instance by tuning the initial BBH so that it is point-symmetric, many of these arrangements are ruled out by the radiated mass constraint (see above and Figure 5).

4. CONCLUSIONS

We conclude that it is extremely unlikely that the LB-1 dark object is currently a black hole binary, or is the remnant of a merger of black holes. The only alternative is that it is a single black hole, formed by direct collapse in an event that shed very little mass. Its existence is therefore a clear challenge to the prediction of envelope ejection caused by pair-instability pulsations, as was already stated in Liu et al. (2019). The findings presented here make it an even stronger case. The single-star collapse scenario for LB-1 might be possible only when a reduction of the stellar wind loss is enforced, as was

shown in Belczynski et al. (2019), albeit with other difficulties there.

We note, moreover, that no significant *sudden* mass loss could have occurred since the system's orbit is currently circular, presumably having experienced tidal circularization, e.g., during a giant phase of the primary star (as inferred in Wolf-Rayet/O-star binaries: Monnier et al. 1999). This includes any pulsation-driven mass loss events, as well as the stellar collapse itself.

The latter is especially interesting in light of the fact that circularization would have spun up the giant's envelope prior to its collapse, leading to the creation of a highly super-Eddington accretion disk during the collapse around the nascent BH. Such disks are thought to re-eject significant fractions of the accreting matter in the form of a disk wind, which may expel additional envelope material (Feng et al. 2018). Clearly in order to maintain a very low orbital eccentricity, none of these effects removed any significant fraction of the object's mass in this case.

REFERENCES

Artymowicz, P., & Lubow, S. H., 1994, ApJ, 421, 651

Barausse, E., Morozova, V., & Rezzolla, L., 2012, ApJ, 758, 63

Belczynski, K.; Hirschi, H.; Kaiser, E. A., et al., Preprint arXiv:1911.12357

Feng, E.-H., Shen, R.-F., & Lin, W.-P. 2018, ApJ, 867, 130

Fitchett, M. J., 1983, MNRAS, 203, 1049

Gerosa, D.; Hébert, F.; Stein, L. C., 2018, Phys. Rev. D, 97, 104049

Healy, J., Lousto, C. O., & Zlochower, Y. 2014, PhRvD, 90, 104004

Monnier, J. D., Tuthill, P. G., & Danchi, W. C. 1999, ApJL, 525, L97

Smak J., 1969, Acta Astromica, 19, 155

Smak J., 1981, Acta Astromica, 31, 395

Horne K., & Marsh T. R., 1986, MNRAS, 218, 761

Huang S.-S., 1972, ApJ, 171, 549

Hummel W., & Dachs J., 1992, A&A, 262, L17

Hummel W, 1994, A&A, 289, 458

Leung S.-C., Nomoto K., Blinnikov S., 2019, Preprint arXiv:1901.11136

Liu, J.-F., Zhang, H.-T., Howard, A., et al., 2019, Nature, 575, 618

Peters, P. C., 1964, Phys. Rev., 136, 1224